

# Conservative Objective Models for Effective Offline Model-Based Optimization

Brandon Trabucco<sup>1</sup> Aviral Kumar<sup>1</sup> Xinyang Geng<sup>1</sup> Sergey Levine<sup>1</sup>

## Abstract

In this paper, we aim to solve data-driven model-based optimization (MBO) problems, where the goal is to find a design input that maximizes an unknown objective function provided access to only a static dataset of inputs and their corresponding objective values. Such data-driven optimization procedures are the only practical methods in many real-world domains where active data collection is expensive (e.g., when optimizing over proteins) or dangerous (e.g., when optimizing over aircraft designs, actively evaluating malformed aircraft designs is unsafe). Typical methods for MBO that optimize the input against a learned model of the unknown score function are affected by erroneous overestimation in the learned model caused due to distributional shift, that drives the optimizer to low-scoring or invalid inputs. To overcome this, we propose *conservative objective models* (COMs), a method that learns a model of the objective function which lower bounds the actual value of the ground-truth objective on out-of-distribution inputs and uses it for optimization. In practice, COMs outperform a number existing methods on a wide range of MBO problems, including optimizing controller parameters, robot morphologies, and superconducting materials.

## 1. Introduction

Black-box model-based optimization (MBO) problems are ubiquitous in a wide range of domains, such as protein (Brookes et al., 2019) or molecule design (Gaulton et al., 2012), designing controllers (Berkenkamp et al., 2016) or robot morphologies (Liao et al., 2019), optimizing neural network designs (Zoph & Le, 2017) and aircraft design (Hoburg & Abbeel, 2012). Existing methods to solve such model-based optimization problems typically learn a

<sup>1</sup>Department of Electrical Engineering and Computer Sciences, University of California Berkeley.. Correspondence to: Brandon Trabucco <btrabucco@berkeley.edu>, Aviral Kumar <aviral@berkeley.edu>.

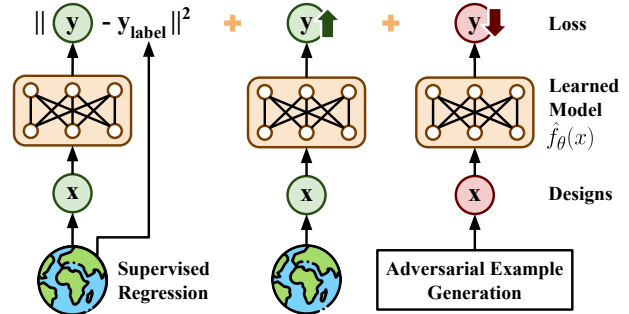


**Figure 1. Overview of COMs.** Our method trains a model of the objective function by training a neural net with supervised regression on the training data augmented two additional loss terms to obtain conservative predictions. These additional terms aim to maximize the predictions of the neural net model on the training data, and minimize the predictions on adversarially generated designs. This principle prevents the optimizer from producing bad designs with erroneously high values at unseen and poor designs.

proxy function to represent the unknown objective landscape based on the data and optimize the design against this learned objective function. In order to prevent errors in the learned proxy function from affecting optimization, these methods often critically rely on a tight interaction loop between optimization and *active* data collection (Snoek et al., 2012). Active data collection can be expensive or even dangerous: evaluating a real design might involve a complex real-world procedure such as synthesizing candidate protein structures for protein optimization or building the robot for robot design optimization. While these problems can potentially be solved via computer simulation, a high fidelity simulator often requires considerable effort from experts across multiple domains to build, making it impractical for most problems. Therefore, a favorable alternative approach for a broad range of MBO problems is to develop *data-driven* methods that can obtain optimized designs by training highly generalizable and expressive deep neural network models on previously collected datasets of inputs ( $x$ ) and their corresponding objective values ( $y$ ), without access to the true function or any form of active data collection (Kumar & Levine, 2019). Moreover, in a number of these practical domains, such as protein (Sarkisyan et al., 2016) or molecule design (Gaulton et al., 2012), plenty of prior data already exists and can be utilized for completely offline model-based optimization.

Typical approaches for addressing MBO problems learn a model of the unknown objective function  $\hat{f}$  that maps an input  $\mathbf{x}$  (Snoek et al., 2012) (or a representation of the input (Gómez-Bombarelli et al., 2018)) to its objective value  $\hat{f}(\mathbf{x})$  via supervised regression, and then optimize the input against this learned model via, for instance, gradient ascent. For MBO problems where the space of valid inputs forms a narrow manifold in a high-dimensional space, any overestimation errors in the learned model will drive the optimization procedure towards off-manifold, invalid, and low-scoring inputs (Kumar & Levine, 2019), as these will falsely appear optimistic under the learned model. Since the offline MBO problem statement does not allow for any active data collection, it is unable to recover from poor solutions which it erroneously predicts high values.

If we can instead learn a *conservative* model of the objective function that does not overestimate the objective value on off-manifold out-of-distribution inputs, optimizing against this conservative model would produce the best solutions for which we are *confident* in the value, thus avoiding going off-manifold or far away from the training data. In this paper, we propose a method to learn such *conservative objective models* (COMs), and then optimize the design against this conservative model using a trust-region constrained gradient-ascent procedure. Building on recent advances in offline reinforcement learning (Levine et al., 2020; Kumar et al., 2020), the key idea behind our method is to train the learned objective function model with an additional objective that minimizes its predictions on out-of-distribution inputs, thus ensuring it does not overestimate the objective value. We show that our approach mitigates overestimation near the manifold of the dataset in theory, and empirically, we find that this leads to good performance across a range of offline model-based optimization tasks.

The primary contribution of this paper is a novel approach for addressing data-driven model-based optimization problems by learning a conservative model of the unknown objective function that lower-bounds the groundtruth function on out-of-distribution inputs, and then optimizing the input against this conservative model via a simple gradient-ascent style procedure. COMs are simple to implement: they only require training a model for the objective function, as opposed to other recent approaches that also train generative models either for generating optimized designs or for estimating the support of the data distribution. We theoretically analyze COMs and show that they never overestimate the values at out-of-distribution inputs close to the dataset manifold and we empirically demonstrate the efficacy of COMs on six complex MBO tasks that span a wide range of real-world tasks including molecule substructure design, neural network parameter optimization, and superconducting material design. On some tasks, COMs outperform the *best* existing method *on that task* by a factor of **1.3-2x**.

## 2. Preliminaries

The goal in data-driven, offline model-based optimization (Kumar & Levine, 2019) is to find best possible solution,  $\mathbf{x}^*$ , to optimization problems of the form

$$\mathbf{x}^* \leftarrow \arg \max_{\mathbf{x}} f(\mathbf{x}), \quad (1)$$

where  $f(\mathbf{x})$  is an unknown (possibly stochastic) objective function. An offline MBO algorithm is provided access to a static dataset  $\mathcal{D}$  of inputs and their objective values,  $\mathcal{D} = \{(\mathbf{x}_1, y_1), \dots, (\mathbf{x}_N, y_N)\}$ . While a variety of MBO methods have been developed (Gómez-Bombarelli et al., 2018; Brookes et al., 2019; Kumar & Levine, 2019; Fan-jiang & Listgarten, 2020), most methods for tackling MBO problems fit a parametric model to the samples of the true objective function in  $\mathcal{D}$ ,  $\hat{f}_\theta(\mathbf{x})$ , via supervised training:  $\hat{f}_\theta(\mathbf{x}) \leftarrow \arg \min_\theta \sum_i (\hat{f}_\theta(\mathbf{x}_i) - y_i)^2$ , and find  $\mathbf{x}^*$  in Equation 1 by optimizing  $\mathbf{x}$  against this learned model  $\hat{f}_\theta(\mathbf{x})$ , typically with some mechanism to additionally minimize distribution shift. One choice for optimizing  $\mathbf{x}$  in Equation 1 is gradient descent on the learned function, as given by

$$\mathbf{x}_{k+1} \leftarrow \mathbf{x}_k + \alpha \nabla_{\mathbf{x}} \hat{f}_\theta(\mathbf{x})|_{\mathbf{x}=\mathbf{x}_k}, \quad \text{for } k \in [1, T], \quad \mathbf{x}^* = \mathbf{x}_T. \quad (2)$$

The fixed point of the above procedure  $\mathbf{x}_T$  is then the output of the MBO procedure. In high-dimensional input spaces, where valid  $\mathbf{x}$  values lie on a thin manifold in a high-dimensional space, such an optimization procedure is prone to producing low-scoring inputs, which may not even be valid. This is because  $\hat{f}$  may erroneously overestimate objective values at out-of-distribution points, which would naturally lead the optimization to such invalid points. Prior methods have sought to address this issue via generative modeling or explicit density estimation, so as to avoid out-of-distribution inputs. In the next section, we will describe how our method, COMs, instead trains the objective model in such a way that overestimation is prevented directly.

## 3. Conservative Objective Models for Offline Model-Based Optimization

In this section, we present our approach, conservative objective models (COMs). COMs learn estimates of the true function that do not overestimate the value of the ground truth objective on out-of distribution inputs in the vicinity of the training dataset. As a result, COMs prevent erroneous overestimation that would drive the optimizer (Equation 2) to produce out-of-distribution and low-scoring inputs. We first discuss a procedure for learning such conservative estimates and then explain how these conservative models can be used for MBO.

### 3.1. Learning conservative objective models (COMs)

The key idea behind our approach is to augment the training of a objective model,  $\hat{f}_\theta(\mathbf{x})$ , typically trained using

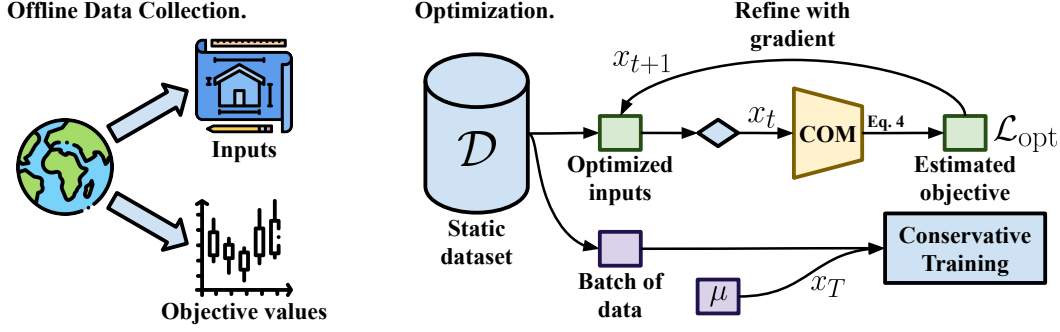


Figure 2. **Training and optimization using COMs.** The section on the left indicates that each task provides a static dataset that is collected offline without any MBO algorithm in-the-loop. The section on the right shows how a conservative objective model is used to produce promising optimized designs using gradient ascent, and how these designs are inputs to a conservative regularizer.

supervised regression, with a regularizer that minimizes the expected value of this function under an automatically chosen adversarial distribution  $\mu(\mathbf{x})$ . We will cover the construction of this adversarial distribution  $\mu(\mathbf{x})$  formally, but intuitively it represents out-of-distribution inputs that are likely to be obtained during optimization and hence their values should be pushed down. While simply minimizing the function values under this adversarial distribution should effectively reduce the learned objective value at these inputs, our approach also additionally maximizes the expected value of this function under  $\hat{D}(\mathbf{x}) = \sum_{\mathbf{x}_i \in \mathcal{D}} \delta_{\mathbf{x}=\mathbf{x}_i}$ , the empirical distribution of the inputs  $\mathbf{x}$  in the dataset  $\mathcal{D}$ . This maximization term prevents excessive underestimation of the learned objective function that can arise *uniformly* over the entire input space when implementing COMs in practice with deep neural network function approximators. In Section 4, we will show that this objective learns a function  $\hat{f}_\theta(\mathbf{x})$  that is a lower bound on the true function  $f(\mathbf{x})$  for inputs that are encountered during the optimization process, under several assumptions. This design is inspired by recent work in offline RL (Kumar et al., 2020), where a similar approach is used to learn conservative value functions, though it has never been applied to MBO to the best of our knowledge. We will elaborate on this connection in Section 5. We will discuss the choice of  $\mu(\mathbf{x})$  in the next paragraph. Formally, our training objective is given by the following equation, where  $\alpha$  is a parameter that trades off conservatism for regression:

$$\hat{f}_\theta^* \leftarrow \arg \min_{\theta \in \Theta} \alpha \left( \mathbb{E}_{\mathbf{x} \sim \mu(\mathbf{x})} [\hat{f}_\theta(\mathbf{x})] - \mathbb{E}_{\mathbf{x} \sim \mathcal{D}} [\hat{f}_\theta(\mathbf{x})] \right) + \frac{1}{2} \mathbb{E}_{(\mathbf{x}, y) \sim \mathcal{D}} \left[ \left( \hat{f}_\theta(\mathbf{x}) - y \right)^2 \right], \quad (3)$$

The value of  $\alpha$  and the choice of distribution  $\mu(\mathbf{x})$  play a crucial role in determining the utility of this bound. If  $\mu(\mathbf{x})$  is not chosen carefully, then the learned function  $\hat{f}_\theta^*$  may not be a lower-bound on the inputs  $\mathbf{x}$  of interest, which is the design actually found by the optimizer. Similarly, if the

chosen  $\alpha$  is very small, then the resulting  $\hat{f}_\theta^*(\mathbf{x})$  may not be a conservative estimate of the actual function  $f(\mathbf{x})$ , whereas if the chosen  $\alpha$  is too large, then the learned function will be too conservative, and not allow the optimizer to deviate away from the dataset at all.

**Choosing  $\mu(\mathbf{x})$ .** Our choice of  $\mu(\mathbf{x})$  specifically focuses on points that the optimizer is likely to encounter while optimizing the input. While there are a number of ways to find such points, the approach we employ is to simply sample a starting point  $\mathbf{x}_0$  from the dataset  $\mathcal{D}$ , and then perform several steps of gradient ascent on  $\hat{f}_\theta$  starting from this point. Since the choice of  $\mu(\mathbf{x})$  depends on  $\theta$ , we reformulate the optimization over  $\theta$  as an *adversarial* optimization problem, as shown below:

$$\hat{f}_\theta^* \leftarrow \arg \min_{\theta \in \Theta} \max_{\mu} \alpha \left( \mathbb{E}_{\mathbf{x} \sim \mu(\mathbf{x})} [\hat{f}_\theta(\mathbf{x})] - \mathbb{E}_{\mathbf{x} \sim \mathcal{D}} [\hat{f}_\theta(\mathbf{x})] \right) + \frac{1}{2} \mathbb{E}_{(\mathbf{x}, y) \sim \mathcal{D}} \left[ \left( \hat{f}_\theta(\mathbf{x}) - y \right)^2 \right].$$

### 3.2. Using COMs for offline model-based optimization

Once we have a trained conservative model from Equation 3, we must use this learned model for finding the best possible input,  $\mathbf{x}^*$ . Prior works (Kumar & Levine, 2019; Brookes et al., 2019) use  $\hat{f}_\theta^*$  in conjunction with generative models or density estimators to restrict the optimization to in-distribution values of  $\mathbf{x}^*$ . However, since our conservative training method trains  $\hat{f}_\theta^*$  to explicitly assign low values to out-of-distribution inputs, we can use a simple gradient-ascent style procedure. Specifically, our optimizer runs gradient-ascent for  $T$  iterations starting from an input in the dataset ( $\mathbf{x}_0 \in \mathcal{D}$ ), in each iteration trying to move the design in the direction of the gradient of the learned model  $\hat{f}_\theta^*$ . However, since our method only prevents overestimation in a given region (specifically, for  $\mathbf{x}$  values drawn from  $\mu(\mathbf{x})$ ), we must make sure that the optimizer doesn't "outrun" this region, since conventional gradient ascent can move very far in even a few steps when gradients are large.

**Algorithm 1** COM: Training Conservative Models

```

1: Initialize  $\hat{f}_\theta$ . Pick  $\eta, \alpha$  and initialize dataset  $\mathcal{D}$ .
2: for  $i = 1$  to training_steps do
3:   Sample  $(\mathbf{x}_0, y) \sim \mathcal{D}$ 
4:   Find  $\mathbf{x}_T(\mathbf{x}_0)$  via gradient ascent from  $\mathbf{x}_0$ :
        $\mathbf{x}_{t+1} = \mathbf{x}_t + \eta \nabla_{\mathbf{x}} \hat{f}_\theta(\mathbf{x})|_{\mathbf{x}=\mathbf{x}_t}; \quad \mu(\mathbf{x}) = \sum_{\mathbf{x}_0 \in \mathcal{D}} \delta_{\mathbf{x}=\mathbf{x}_T(\mathbf{x}_0)}$ .
5:   Minimize  $\mathcal{L}(\theta; \alpha)$  with respect to  $\theta$ .
        $\mathcal{L}(\theta; \alpha) = \mathbb{E}_{\mathbf{x}_0 \sim \mathcal{D}} (\hat{f}_\theta(\mathbf{x}_0) - y)^2 - \alpha \mathbb{E}_{\mathbf{x}_0} [\hat{f}_\theta(\mathbf{x}_0)] + \alpha \mathbb{E}_{\mu(\mathbf{x})} [\hat{f}_\theta(\mathbf{x})]$ 
        $\theta \leftarrow \theta - \lambda \nabla_{\theta} \mathcal{L}(\theta; \alpha)$ 
6: end for
    
```

**Algorithm 2** COM: Finding  $\mathbf{x}^*$ 

```

1: Initialize optimizer at the optimum in  $\mathcal{D}$ :
    $\tilde{\mathbf{x}} = \arg \max_{(\mathbf{x}, y) \in \mathcal{D}} y$ 
2: Find  $\mathbf{x}^*$  via trust-region gradient ascent from  $\tilde{\mathbf{x}}$ :
    $\mathbf{x}_{t+1} = \mathbf{x}_t + \eta \nabla_{\mathbf{x}} \mathcal{L}_{\text{opt}}(\mathbf{x})|_{\mathbf{x}=\mathbf{x}_t}$ 
   where  $\mathcal{L}_{\text{opt}}(\mathbf{x}) := \hat{f}_\theta^*(\mathbf{x}) - \beta \hat{f}_\theta^*(\mathbf{x} + \eta \nabla_{\mathbf{x}} \hat{f}_\theta^*(\mathbf{x}))$ .
3: Return the solution  $\mathbf{x}^* = \mathbf{x}_T$ .
    
```

We therefore incorporate a “trust-region” constraint into our optimizer. Starting from the best point in the dataset,  $\mathbf{x}_0 \in \mathcal{D}$ , our optimizer performs the following update (also shown in Algorithm 2, Line 2):

$$\forall t \in [T], \mathbf{x}_0 \in \mathcal{D}; \quad \mathbf{x}_{t+1} = \mathbf{x}_t + \eta \nabla_{\mathbf{x}} \mathcal{L}_{\text{opt}}(\mathbf{x})|_{\mathbf{x}=\mathbf{x}_t}$$

where  $\mathcal{L}_{\text{opt}}(\mathbf{x}) := \hat{f}_\theta^*(\mathbf{x}) - \beta \hat{f}_\theta^*(\mathbf{x} + \eta \nabla_{\mathbf{x}} \hat{f}_\theta^*(\mathbf{x}))$ . (4)

Equation 4 ensures that the value of the learned function  $\hat{f}_\theta(\mathbf{x}_{t+1})$  is larger than the value at its previous iterate  $\mathbf{x}_t$  and it additionally penalizes the value at a hallucinated, lookahead gradient-ascent iterate beyond  $\mathbf{x}_{t+1}$  weighted by  $\beta$ . This  $\beta$ -weighted penalty ensures that the function  $\hat{f}_\theta(\mathbf{x})$  is relatively constant near the obtained  $\mathbf{x}_{t+1}$ , and is expected to decrease the rate at which naïve gradient ascent can outrun the region defined by  $\mu(\mathbf{x})$  in Equation 3, that the conservative model was trained on.

Equation 4 is theoretically equivalent (upto second order) to standard gradient ascent on learned  $\hat{f}^*(\mathbf{x})$ , with an additional regularizer on the norm of the gradient  $\nabla_{\mathbf{x}} \hat{f}^*(\mathbf{x})$  (to observe this note the Taylor expansion of  $\mathcal{L}_{\text{opt}}(\mathbf{x})$  in Equation 4). Thus, it implements a “slow” version of gradient ascent such that  $\mathbf{x}^*$  doesn’t outrun the region during optimization. A detailed discussion of this constraint along with how it is implemented in practice is provided in Appendix A.

### 3.3. Additional Design Decisions for COMs

Next we discuss other design decisions that appear in COMs training (Equation 3) or when optimizing the input against a learned conservative model (Equation 4).

**Choosing  $\alpha$ .** The hyperparameter  $\alpha$  in Equation 3 plays an important role in weighting conservatism against accuracy. Without access to additional active data collection for evaluation, tuning this hyperparameter for each task can be challenging. Therefore, in order to turn COMs into a task-agnostic algorithm for offline MBO, we devise an automated procedure for selecting  $\alpha$ . As discussed previously, if  $\alpha$  is too large,  $\hat{f}_\theta^*$  is expected to be too conservative, since it would assign higher values to points in the dataset, and low values to *all* other points. Selecting a single value of  $\alpha$  that works for many problems is difficult, since its effect

depends strongly on the magnitude of the objective function. Instead, we use a modified training procedure that poses Equation 3 as a constrained optimization problem, with  $\alpha$  assuming the role of a Lagrange dual variable for satisfying a constraint that controls the difference in values of the learned objective under  $\mu(\mathbf{x})$  and  $\mathcal{D}(\mathbf{x})$ . This corresponds to solving the following optimization problem:

$$\begin{aligned} \hat{f}_\theta^* \leftarrow \arg \min_{\theta \in \Theta} \frac{1}{2} \mathbb{E}_{(\mathbf{x}, y) \sim \mathcal{D}} \left[ \left( \hat{f}_\theta(\mathbf{x}) - y \right)^2 \right] \\ \text{s.t.} \quad \left( \mathbb{E}_{\mathbf{x} \sim \mu(\mathbf{x})} [\hat{f}_\theta(\mathbf{x})] - \mathbb{E}_{\mathbf{x} \sim \mathcal{D}} [\hat{f}_\theta(\mathbf{x})] \right) \leq \tau. \end{aligned} \quad (5)$$

While Equation 5 introduces a new hyperparameter  $\tau$  in place of  $\alpha$ , this parameter is easier to select by hand, since its optimal value does not depend on the magnitude of the objective function (as objective values are normalized before use in Equation 5), and therefore a single choice works well across a range of tasks. We find that a single value of  $\tau = 0.05$  is effective on every task and empirically ablate the choice of  $\tau$  in Appendix A.

**Selecting optimized designs  $\mathbf{x}^*$ .** So far we have discussed how COMs can be trained and used for optimization; however, we have not established a way to determine which  $\mathbf{x}_t$  (Equation 4) encountered in the optimization trajectory should be used as our final solution  $\mathbf{x}^*$ . The most natural choice is to pick the final  $\mathbf{x}_T$  found by the optimizer as the solution. On all of our tasks, we choose  $T$  to be a large value equal to 450 steps. While the choice of  $T$  should, in principle, affect the solution found by any gradient-ascent style optimizer, we found COMs to be quite stable to different values of  $T$ , as we will elaborate empirically on in Section 6.2, Figure 3. Of course, there are many other possible ways of selecting  $T$ , including ideas inspired from offline model-selection methods in offline reinforcement learning (Thomas et al., 2015), but our simple procedure, which is also popular in offline RL (Fu et al., 2020), is sufficient to obtain good optimization performance.

**Choice of  $\mu(\mathbf{x})$ .** By default, we compute  $\mu(\mathbf{x})$  via multiple steps of gradient ascent on the learned  $\hat{f}(\mathbf{x})$  during training, which is different from the procedure for computing  $\mathbf{x}^*$  in Equation 4, we find that a version of COMs that also uti-



lizes the trust-region procedure in Equation 4 for computing  $\mu(\mathbf{x})$  in Equation 3 also performs similarly to this default version of COMs. We present empirical evidence for this observation in Appendix A.

### 3.4. Overall Algorithm and Practical Implementation

Finally, we combine the individual components discussed so far to obtain a complete algorithm for offline model-based optimization. Pseudocode for our algorithm is shown in Algorithm 1. COMs parameterize the objective model,  $\hat{f}_\theta(\mathbf{x})$ , via a feed-forward neural network with parameters  $\theta$ . Our method then alternates between approximately generating samples  $\mu(\mathbf{x})$  via gradient ascent (Line 4), and optimizing parameters  $\theta$  using Equation 4 (Line 5). Finally, at the end of training, we run the trust-region gradient ascent procedure over the learned objective model  $\hat{f}_\theta^*(\mathbf{x})$  for a large  $T$  number of ascent steps and return the final design  $\mathbf{x}_T$  as  $\mathbf{x}^*$ .

**Implementation details.** Elaborate implementation details for our method can be found in Appendix A. Briefly, for all of our experiments, the conservative objective model  $\hat{f}_\theta$  is modeled as a neural network with two hidden layers of size 2048 each and leaky ReLU activations. More details on the network structure can be found in Appendix C. In order to train this conservative objective model, we use the Adam optimizer (Kingma & Ba, 2015) with a learning rate of  $10^{-3}$ . Empirically, we found larger values of  $\eta$  to produce inputs  $\mathbf{x}_T$  that do not maximize the values of  $\hat{f}_\theta^*(\mathbf{x}_T)$ , and we select the largest  $\eta$  such that successive  $\mathbf{x}_t$  follow the gradient vector field of  $\hat{f}_\theta^*(\mathbf{x}_t)$ . For computing samples  $\mu(\mathbf{x})$ , we used one gradient ascent step starting from a given design in the dataset,  $\mathbf{x}_0 \in \mathcal{D}$ . While it appears limiting at first, we show in Appendix A that this is sufficient to ensure the conservatism constraint in Equation 5. During optimization, we utilized the trust-region gradient-ascent optimizer with  $\beta = 0.9$ . As we will also show in our experiments (Section 6.2), this value of  $\beta$  universally produces stable optimization behavior. Finally, in order to choose the time step  $T$  in Equation 4 that is supposed to provide us with the final solution  $\mathbf{x}^* = \mathbf{x}_T$ , we pick a large and universal time step of  $T = 450$ .

## 4. Theoretical Analysis of COMs

We will now theoretically analyze conservative objective models, and show that the conservative training procedure (Equation 3) indeed learns a conservative model of the objective function. To do so, we will show that under Equation 3, the values of all inputs in regions found within  $T$  steps of gradient ascent starting from any input  $\mathbf{x}_0 \in \mathcal{D}$  are lower-bounds on their actual value. For analysis, we shall denote  $\bar{\mathcal{D}}(\mathbf{x})$  as the smoothed density of  $\mathbf{x}$  in the dataset  $\mathcal{D}$  (see Appendix B for a formal definition). We will express Equation 3 in an equivalent form that factorizes the distribution

$\mu(\mathbf{x})$  as  $\mu(\mathbf{x}) = \sum_{\mathbf{x}_0 \sim \mathcal{D}} \bar{\mathcal{D}}(\mathbf{x}_0) \mu(\mathbf{x}_T | \mathbf{x}_0)$ :

$$\min_{\theta \in \Theta} \alpha \left( \mathbb{E}_{\mathbf{x}_0 \sim \bar{\mathcal{D}}, \mathbf{x}_T \sim \mu(\mathbf{x}_T | \mathbf{x}_0)} [\hat{f}_\theta(\mathbf{x}_T)] - \mathbb{E}_{\mathbf{x} \sim \bar{\mathcal{D}}} [\hat{f}_\theta(\mathbf{x})] \right) + \frac{1}{2} \mathbb{E}_{(\mathbf{x}, y) \sim \bar{\mathcal{D}}} \left[ \left( \hat{f}_\theta(\mathbf{x}) - y \right)^2 \right]. \quad (6)$$

While  $\mu(\mathbf{x}_T | \mathbf{x}_0)$  is a Dirac-delta distribution in practice (Section 3), for our analysis, we will assume that it is a distribution centered at  $\mathbf{x}_T$  and  $\mu(\mathbf{x}_T | \mathbf{x}_0) > 0 \forall \mathbf{x}_T \in \mathcal{X}$ . This condition can be easily satisfied by adding random noise during gradient ascent while computing  $\mathbf{x}_T$ . We will train  $\hat{f}_\theta$  using gradient descent and denote  $k = 1, 2, \dots$  as the iterations of this training procedure for  $\hat{f}_\theta$ .

We first summarize some assumptions used in our analysis. We assume that the true function  $f(\mathbf{x})$  is  $L$ -Lipschitz over the input space  $\mathbf{x}$ . We also assume that the learned function  $\hat{f}_\theta(\mathbf{x})$  is  $\hat{L}$ -Lipschitz and  $\hat{L}$  is sufficiently larger than  $L$ . For analysis purposes, we will define a conditional distribution,  $\bar{\mathcal{D}}(\mathbf{x}' | \mathbf{x})$ , to be a Gaussian distribution centered at  $\mathbf{x}$ :  $\mathcal{N}(\mathbf{x}' | \mathbf{x}, \sigma^2)$ . We will not assume a specific parameterization for the objective model,  $\hat{f}_\theta$ , but operate under the neural tangent kernel (NTK) (Jacot et al., 2018) model of neural nets. The neural tangent kernel of the function  $\hat{f}(\mathbf{x})$  be defined as:  $\mathbf{G}_f(\mathbf{x}_i, \mathbf{x}_j) := \nabla_{\theta} \hat{f}_\theta(\mathbf{x}_i)^T \nabla_{\theta} \hat{f}_\theta(\mathbf{x}_j)$ . Under these assumptions, we build on the analysis of conservative Q-learning (Kumar et al., 2020) to prove our theoretical result in Theorem 1, shown below:

**Proposition 1** (Conservative training lower-bounds the true function). *Assume that  $\hat{f}_\theta(\mathbf{x})$  is trained with conservative training by performing gradient descent on  $\theta$  with respect to the objective in Equation 6 with a learning rate  $\eta$ . The parameters in step  $k$  of gradient descent are denoted by  $\theta^k$ , and let the corresponding conservative model be denoted as  $\hat{f}_\theta^k$ . Let  $\mathbf{G}$ ,  $\mu$ ,  $\hat{L}$ ,  $L$ ,  $\bar{\mathcal{D}}$  be defined as discussed above. Then, under assumptions listed above,  $\forall \mathbf{x} \in \mathcal{D}, \mathbf{x}' \in \mathcal{X}$ , the conservative model at iteration  $k + 1$  of training satisfies:*

$$\begin{aligned} \hat{f}_\theta^{k+1}(\mathbf{x}'') := \max \bigg\{ & \hat{f}_\theta^{k+1}(\mathbf{x}) - \hat{L} \|\mathbf{x}'' - \mathbf{x}\|_2, \\ & \hat{f}_\theta^{k+1}(\mathbf{x}'') - \eta \alpha \mathbb{E}_{\mathbf{x} \sim \bar{\mathcal{D}}, \mathbf{x}' \sim \mu} [\mathbf{G}_f^k(\mathbf{x}'', \mathbf{x}')] \\ & + \eta \alpha \mathbb{E}_{\mathbf{x} \sim \bar{\mathcal{D}}, \mathbf{x}' \sim \bar{\mathcal{D}}} [\mathbf{G}_f^k(\mathbf{x}'', \mathbf{x}')] \bigg\}, \end{aligned}$$

where  $\hat{f}_\theta^{k+1}(\mathbf{x}'')$  is the resulting  $(k+1)$ -th iterate of  $\hat{f}_\theta$  if conservative training were not used. Thus, if  $\alpha$  is sufficiently large, the expected value of the asymptotic function,  $\hat{f}_\theta := \lim_{k \rightarrow \infty} \hat{f}_\theta^k$ , on inputs  $\mathbf{x}_T$  found by the optimizer, lower-bounds the value of the true function  $f(\mathbf{x}_T)$ :

$$\mathbb{E}_{\mathbf{x}_0 \sim \mathcal{D}, \mathbf{x}_T \sim \mu(\mathbf{x}_T | \mathbf{x}_0)} [\hat{f}_\theta(\mathbf{x}_T)] \leq \mathbb{E}_{\mathbf{x}_0 \sim \mathcal{D}, \mathbf{x}_T \sim \mu(\mathbf{x}_T | \mathbf{x}_0)} [f(\mathbf{x})].$$

A proof for Proposition 1 including a complete formal statement can be found in Appendix B. The intuition behind

the proof is that inducing conservatism in the function  $\hat{f}_\theta$  at each gradient step of optimizing Equation 6 makes the asymptotic function be conservative. Moreover, the larger the value of  $\alpha$ , the more conservative the function  $\hat{f}_\theta$  is on points  $\mathbf{x}'$  found via gradient ascent, i.e., points with high density under  $\mu(\mathbf{x}_T|\mathbf{x}_0)$ , in expectation. Finally, when gradient ascent is used to find  $\mathbf{x}^*$  on the learned conservative model,  $\hat{f}_\theta$ , and the number of steps of gradient ascent steps is less than  $T$ , this bound with an offset to account for the fact that the bound in Proposition 1 is computed in expectation over  $\mathbf{x}_T$  while we want to bound the point  $\mathbf{x}^*$ , will hold for the point  $\mathbf{x}^*$ , and therefore the estimated value of this point will not overestimate its true value. This offset depends on the Lipschitz constant  $\hat{L}$  and the distance between  $\mathbf{x}^*$  and the optimized solutions  $\mathbf{x}_T$  found for other data points,  $\mathbf{x}_0 \in \mathcal{D}$ .

## 5. Related Work

We now briefly discuss prior works in MBO, including prior work on active model-based optimization and work that utilizes offline datasets for data-driven MBO.

**Bayesian optimization.** Most prior work on model-based optimization has focused on the active setting, where derivative free methods such as the cross-entropy method (Rubinstein & Kroese, 2004) and other methods derived from the REINFORCE trick (Williams, 1992b; Rubinstein, 1996), reward-weighted regression (Peters & Schaal, 2007), and Gaussian processes (Snoek et al., 2015; Shahriari et al., 2016; Snoek et al., 2012) have been utilized. Most of these methods focus mainly on low-dimensional tasks with active data collection. Practical approaches have combined these methods with Bayesian neural networks (Snoek et al., 2015; 2012), latent variable models (Kim et al., 2019; Garnelo et al., 2018b;a), and ensembles of learned score models (Angermueller et al., 2020a;b; Mirhoseini et al., 2020). These methods still require actively querying the true function  $f(\mathbf{x})$ . Further, as shown by (Brookes et al., 2019; Fannjiang & Listgarten, 2020; Kumar & Levine, 2019), these Bayesian optimization methods are susceptible to producing invalid out-of-distribution inputs in the offline setting. Unlike these methods, COMs are specifically designed for the offline setting with high-dimensional inputs, and avoid out-of-distribution inputs.

**Offline model-based optimization.** Recent works have also focused on optimization in the completely offline setting. Typically these methods utilize a generative model (Kingma & Welling, 2013; Goodfellow et al., 2014a) that models the manifold of inputs. (Brookes et al., 2019; Fannjiang & Listgarten, 2020) use a variational autoencoder (Kingma & Welling, 2013) to model the space of  $\mathbf{x}$  and use it alongside a learned objective function. (Kumar & Levine, 2019) use a generative model to parameterize

an inverse map from the scalar objective  $y$  to input  $\mathbf{x}$  and search for the optimal one-dimensional  $y$  during optimization. Modeling the manifold of valid inputs globally can be extremely challenging (see Ant, Hopper, and DKitty results in Section 6), and as a result these generative models often need to be tuned for each domain (Trabucco et al., 2021). In contrast, COMs do not require any generative model, and fit an approximate objective function with a simple regularizer, providing both a simpler, easier-to-use algorithm and better empirical performance.

**Adversarial examples.** As discussed in Section 2, MBO methods based on learned objective models naturally query the learned function on “adversarial” inputs, where the learned function erroneously overestimates the true function. This is superficially similar to adversarial examples in supervised learning (Goodfellow et al., 2014b), which can be generated by maximizing the input against the loss function. While adversarial examples have been formalized as out-of-distribution inputs lying in the vicinity of the data distribution and prior works have attempted to correct for them by encouraging smoothness (Tramèr et al., 2018) of the learned function, and there is evidence that robust objective models help mitigate over estimation (Santurkar et al., 2019), these solutions may be ineffective in MBO settings when the true function is itself non-smooth. Instead making conservative predictions on such adversarially generated inputs may prevent poor performance.

## 6. Experimental Evaluation

To evaluate the efficacy of COMs for offline model-based optimization, we first perform a comparative evaluation of COMs on four continuous offline MBO tasks based on problems in physical sciences, neural network design, and robotics, proposed in the design-bench benchmark (Trabucco et al., 2021). In addition, we perform an empirical analysis on COMs that aims to answer the following questions: (1) Is conservative training essential for improved performance and stability of COMs? How do COMs compare to a naïve objective model in terms of stability?, (2) How does the trust-region optimizer improve the stability of optimizing COMs?, (3) Are COMs robust to hyperparameter choices and consistent to evaluation conditions? We answer these questions by studying the behavior of COMs under controlled conditions by using visualizations for our analysis. Code for reproducing our experimental results is available at <https://github.com/brandontrabucco/design-baselines>.

### 6.1. Empirical Performance on Benchmark Tasks

We first compare COMs to a range of recently proposed methods for offline MBO in high-dimensional input spaces: CbAS (Brookes et al., 2019), MINs (Kumar & Levine,

$\mathcal{D}$ (best)	Superconductor-v0 73.90	HopperController-v0 1361.6	AntMorphology-v0 108.5	DKittyMorphology-v0 215.9
MINs	80.23 $\pm$ 10.67	746.1 $\pm$ 636.8	388.5 $\pm$ 9.085	352.9 $\pm$ 38.65
CbAS	72.17 $\pm$ 8.652	547.1 $\pm$ 423.9	393.0 $\pm$ 3.750	369.1 $\pm$ 60.65
Autofocus	77.07 $\pm$ 11.11	443.8 $\pm$ 142.9	386.9 $\pm$ 10.58	376.3 $\pm$ 47.47
Grad. Ascent	89.64 $\pm$ 9.201	1050.8 $\pm$ 284.5	399.9 $\pm$ 4.941	<b>390.7 <math>\pm</math> 49.24</b>
REINFORCE	86.58 $\pm$ 4.270	553.0 $\pm$ 296.0	<b>446.3 <math>\pm</math> 8.669</b>	334.5 $\pm$ 38.22
CMA-ES	98.59 $\pm$ 5.271	676.5 $\pm$ 344.5	<b>921.3 <math>\pm</math> 1383.</b>	-0.9 $\pm$ 2.350
BO-qEI	89.73 $\pm$ 0.000	759.4 $\pm$ 142.3	348.6 $\pm$ 4.229	265.5 $\pm$ 0.000
COMs (ours)	<b>114.47 <math>\pm</math> 6.400</b>	<b>2149.5 <math>\pm</math> 400.3</b>	<b>442.4 <math>\pm</math> 9.651</b>	333.4 $\pm$ 32.16

Table 1. **Comparative evaluation of COMs** against prior methods in terms of the mean 100th-percentile score and its standard deviation over 16 trials. Tasks include Superconductor-v0, HopperController-v0, AntMorphology-v0, and DKittyMorphology-v0, which is the set of continuous tasks provided by (Trabucco et al., 2021). COMs perform strictly better on high-dimensional tasks, obtaining about **2x** gains on HopperController-v0, and compelling gains on Superconductor-v0 and AntMorphology-v0 tasks. In addition, COMs is the only method that is able to consistently find solutions that outperform the best training point for each task, given by  $\mathcal{D}$  (best). For each task, algorithms within one standard deviation of having the highest performance are bolded.

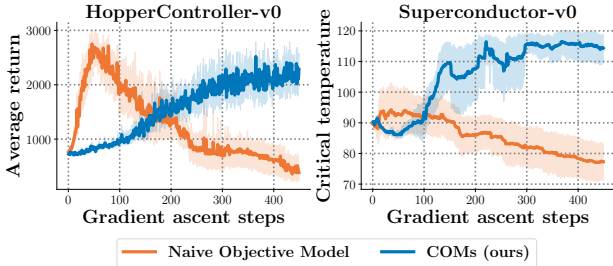


Figure 3. **Stability of COMs versus naïve gradient ascent.** The x-axis shows the number of gradient ascent steps taken on the design  $\mathbf{x}^*$ , and the y-axis shows the 100th percentile of the ground truth task objective function evaluated at every gradient step, which is used only for analysis only and is unavailable to the algorithm. In both cases, COMs reach solutions that remain at higher performance stably, indicating that COMs are less sensitive to varying numbers of gradient ascent steps performed during optimization.

2019), REINFORCE (Williams, 1992a), CMA-ES (Hansen, 2006) and autofocused CbAS (Fannjiang & Listgarten, 2020), that augments CbAS with a re-weighted objective model, and BO-qEI, Bayesian Optimization with the quasi-expected improvement acquisition function (Wilson et al., 2017). CbAS and MINs train generative models such as VAEs (Kingma & Welling, 2013) and GANs (Goodfellow et al., 2014a), which generally require task-specific neural net architectures, as compared to the substantially simpler discriminative models used for COMs. In fact, we use the same architecture for COMs in all experiments and for all tasks. We also compare to a naïve gradient ascent baseline that simply learns a non-conservative model of the objective and optimizes against it via gradient ascent.

Our evaluation protocol follows prior work (Brookes et al., 2019; Trabucco et al., 2021): we query each method to obtain the top  $N = 128$  most promising optimized samples  $\mathbf{x}_1^*, \dots, \mathbf{x}_N^*$  according to the model, and then report the 100<sup>th</sup> percentile ground truth objective values on this set of

samples,  $\max(\mathbf{x}_1^*, \dots, \mathbf{x}_N^*)$ , as well as the 50<sup>th</sup> percentile objective value, averaged over 16 trials. We would argue that such an evaluation scheme is reasonable as it is typically followed in real-world MBO problems, where a set of optimized inputs are produced by the model, and the best performing one of them is finally used for deployment.

Our results for different domains are shown in Table 1: (A) Superconductor-v0 (Fannjiang & Listgarten, 2020), where the goal is to optimize over 81-dimensional superconductor designs to maximize the critical temperature using 16953 points, (B) HopperController-v0 (Kumar & Levine, 2019), where the goal is to optimize over 5126-dimensional weights of a neural network policy on the Hopper-v2 gym domain using a dataset of 3200 points, and (C) Ant and (D) DKittyMorphology-v0, where the goal is to design the 60 and 56-dimensional morphology, respectively, of robots to maximize policy performance using datasets of size 12300 and 9546, respectively. Results for baseline methods are based on numbers reported by Trabucco et al. (2021). Additional details for the setup of these tasks is provided in Appendix Section D. On three out of four tasks, COMs attain the best results, in some cases (e.g. (B) HopperController) attaining the performance of over *twice* the best prior method. In addition, COMs are shown to be the only method to attain higher performance than the best training point on every task. While COMs performs within a standard deviation margin of CbAS and MINs on DKittyMorphology-v0, it substantially outperforms prior methods on Superconductor-v0 and the high-dimensional HopperController-v0 tasks, by a factor of **1.3-2x**. A naïve objective model without the conservative term, which is prone to falling off-the-manifold of valid inputs, struggles in especially high-dimensional tasks. These results indicate that COMs can serve as simple yet powerful method for offline MBO across a variety of domains. Furthermore, note that COMs only require training



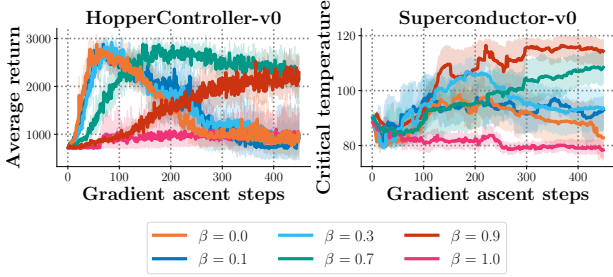


**Figure 4. Ablation of stability and universality of  $\beta$ .** In each of the two plots, we instantiate COMs on the HopperController-v0 and Superconductor-v0 tasks, and vary  $\beta$  that controls the strength of the trust-region (Equation 4). The x-axis denotes the number of gradient ascent steps taken on the design  $\mathbf{x}^*$  with respect to  $\hat{f}_\theta$ , and the y-axis indicates the 100th percentile of the ground truth function  $\mathbf{x}$ , which remains unobserved by the COMs algorithm, and only serves as an ablative visualization. The results demonstrate that increasing  $\beta$  results in improved stability of COMs, and *universally*,  $\beta = 0.9$  results in consistent high performance.

a parametric model  $y = \hat{f}_\theta(x)$  of the objective function with a regularizer, without any need for training a generative model, which may be harder in practice to tune.

## 6.2. Ablation Studies

In this section, we perform an ablative experimental analysis of COMs to answer questions posed at the beginning of Section 6. First, we evaluate the efficacy of using conservative training for learning a model of the objective function by comparing COMs to a naïve gradient ascent baseline and show that COMs are more *stable*, i.e., the optimization performance of COMs is much less sensitive to the number of gradient ascent steps used for optimization. Second, we evaluate the effect of the value of  $\beta$  (Equation 4) that controls the strength of the trust-region constraint and show that a single  $\beta$  is uniformly optimal on a wide-variety of MBO tasks over input spaces with very distinct properties. Finally, we demonstrate the *consistency* of COMs by evaluating the sensitivity of the optimization performance with respect to the number of samples  $N$ , that are used to compute the evaluation metric  $\max(\mathbf{x}_1^*, \dots, \mathbf{x}_N^*)$ .

**COMs are more stable than naïve gradient ascent.** In order to better compare COMs and a naïve objective model optimized using gradient ascent, we visualize the true objective value for each  $\mathbf{x}_t$  encountered during optimization ( $t$  in Line 2, Algorithm 2) in Figure 3. Observe that a naïve objective model can attain good performance for a “hand-tuned” number of gradient ascent steps, but it soon degrades in performance with more steps. This indicates that COMs are much more stable to the choice of number of gradient ascent steps performed than a naïve objective model.

**Trust-region gradient-ascent (Equation 4) improves stability and COMs are robust to  $\beta$ .** Next we evaluate the

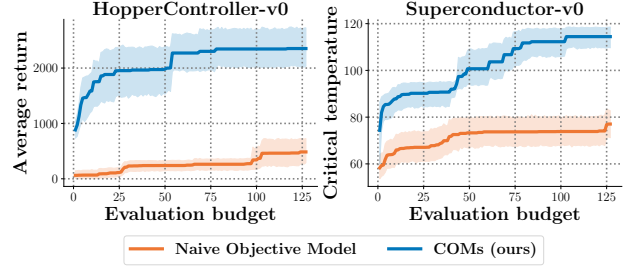


**Figure 5. Ablation of consistency of COMs by visualizing sensitivity to the post-optimization evaluation budget.** How does the performance of COMs and naïve gradient ascent vary as the evaluation budget is reduced? In our standard evaluation, we allow each offline MBO algorithm a “budget” of 128 evaluations for determining 100th and 50th percentile performance. The x-axis indicates the number  $N$  of allowed evaluations, and the y-axis indicates the 100th percentile performance of the chosen  $N$  points. As this evaluation budget is reduced, COMs is resilient, and remains superior to the naïve objective trained via supervised regression and optimized via standard gradient ascent. In the case of HopperController-v0, COMs is nearly invariant to budgets down to size 55. This indicates that COMs consistently produce optimized inputs  $\mathbf{x}^*$  that attain high values under the true function.

stability of COMs to the various values of the hyperparameter  $\beta$  that appears in the trust-region gradient-ascent optimization (Equation 4). Note that this  $\beta$  was chosen universally across tasks. In Figure 4, we evaluate the sensitivity of the performance of COMs with respect to  $\beta$  on two tasks: HopperController-v0, and Superconductor-v0. Note that in both cases, COMs becomes increasingly stable and performance improves as  $\beta$  approaches an upper limit of 1, and appears optimal in both tasks for  $\beta = 0.9$ . While COMs do not completely eliminate this hyperparameter, our empirical results in Table 1 across a wide-array of input types (*both* the weights of a neural network in HopperController and the morphology of a robot in AntMorphology; 60 dimensions vs 5126 dimensional input spaces; etc.) with  $\beta = 0.9$  suggest this value is universal and can be fixed to a constant.

**COMs consistently produce well-performing inputs.** Finally, we evaluate the sensitivity of COMs to the evaluation procedure itself. Standard evaluation practice in offline MBO dictates evaluating a batch of  $N$  most promising candidate inputs produced by the algorithm with the ground truth objective, where  $N$  remains constant across all algorithms (Trabucco et al., 2021; Brookes et al., 2019), and using the maximum value attained over these inputs as the performance of the algorithm, i.e.,  $\max(\mathbf{x}_1^*, \dots, \mathbf{x}_N^*)$ . This measures if the algorithm performs well within a provided “evaluation budget” of  $N$  evaluations. An algorithm is more *consistent* if it attains higher values of the groundtruth function with a smaller value of the evaluation budget,  $N$ . We used  $N = 128$  for evaluating all methods in Table 1, but the value of  $N$  is technically a hyperparameter and an effective



offline MBO method should be resilient to this value, ideally. COMs are resilient to  $N$ : as we vary  $N$  from 1 to 128 in Figure 5, COMs not only perform well at larger values of  $N$ , but are also effective with smaller budgets, reaching near-optimal performance on HopperController-v0 in with a budget of 55, while a naïve objective model needs a budget twice as large to reach its own optimal performance, which is lower than that of COMs.

## 7. Discussion and Conclusion

We proposed conservative objective models (COM), a simple method for offline model-based optimization, that learns a conservative estimate of the actual objective function and optimizes the input against this estimate. Empirically, we find that COMs give rise to good offline optimization performance and are considerably more stable than prior MBO methods, returning solutions that are comparable to and even better than the best existing MBO algorithms on four benchmark tasks. In this evaluation, COMs are consistently high performing, and in the most high-dimensional cases, COMs improves on the next best method by a factor of **1.3-2x**. The simplicity of COMs combined with their empirical strength make them a promising optimization backbone to find solutions to challenging and high-dimensional offline MBO problems. In contrast to certain prior methods, COMs are designed to mitigate overestimation of out-of-distribution inputs close to the input manifold, and show improved stability once good solutions are found.

While our results suggest that COMs are effective on a number of MBO problems, there exists room for improvement. The somewhat naïve gradient-ascent optimization procedure employed by COMs can likely be improved by combining it with manifold modelling techniques, which can accelerate optimization by alleviating the need to traverse the raw input space. Similar to offline RL and supervised learning, learned objective models in MBO are prone to overfitting, especially in limited data settings. Understanding different mechanisms by which overfitting can happen and correcting for it is likely to greatly amplify the applicability of COMs to a large set of practical MBO problems that only come with small datasets. Understanding why and how samples found by gradient ascent become off-manifold could result in a more powerful gradient-ascent optimization procedure that does not require a model-selection scheme.

## Acknowledgements

We thank anonymous reviewers and all other members from RAIL at UC Berkeley for their suggestions, feedback and support. This work was supported by National Science Foundation and the DARPA Assured Autonomy Program, and compute support from Google and Intel.

## References

- Angermueller, C., Belanger, D., Gane, A., Mariet, Z., Dohan, D., Murphy, K., Colwell, L., and Sculley, D. Population-based black-box optimization for biological sequence design. *arXiv preprint arXiv:2006.03227*, 2020a.
- Angermueller, C., Dohan, D., Belanger, D., Deshpande, R., Murphy, K., and Colwell, L. Model-based reinforcement learning for biological sequence design. In *International Conference on Learning Representations*, 2020b. URL <https://openreview.net/forum?id=HklxbgBKvr>.
- Berkenkamp, F., Schoellig, A. P., and Krause, A. Safe controller optimization for quadrotors with gaussian processes. In *2016 IEEE International Conference on Robotics and Automation (ICRA)*, pp. 491–496. IEEE, 2016.
- Brookes, D., Park, H., and Listgarten, J. Conditioning by adaptive sampling for robust design. In *Proceedings of the 36th International Conference on Machine Learning*. PMLR, 2019. URL <http://proceedings.mlr.press/v97/brookes19a.html>.
- Fannjiang, C. and Listgarten, J. Autofocused oracles for model-based design. *arXiv preprint arXiv:2006.08052*, 2020.
- Fu, J., Kumar, A., Nachum, O., Tucker, G., and Levine, S. D4rl: Datasets for deep data-driven reinforcement learning, 2020.
- Garnelo, M., Rosenbaum, D., Maddison, C., Ramalho, T., Saxton, D., Shanahan, M., Teh, Y. W., Rezende, D., and Eslami, S. M. A. Conditional neural processes. In *Proceedings of the 35th International Conference on Machine Learning*. PMLR, 2018a.
- Garnelo, M., Schwarz, J., Rosenbaum, D., Viola, F., Rezende, D. J., Eslami, S. M. A., and Teh, Y. W. Neural processes. *CoRR*, abs/1807.01622, 2018b. URL <http://arxiv.org/abs/1807.01622>.
- Gaulton, A., Bellis, L. J., Bento, A. P., Chambers, J., Davies, M., Hersey, A., Light, Y., McGlinchey, S., Michalovich, D., Al-Lazikani, B., et al. ChEMBL: a large-scale bioactivity database for drug discovery. *Nucleic acids research*, 40(D1):D1100–D1107, 2012.
- Gómez-Bombarelli, R., Duvenaud, D., Hernández-Lobato, J. M., Aguilera-Iparraguirre, J., Hirzel, T. D., Adams, R. P., and Aspuru-Guzik, A. Automatic chemical design using a data-driven continuous representation of molecules. In *ACS central science*, 2018.

- Goodfellow, I. J., Pouget-Abadie, J., Mirza, M., Xu, B., Warde-Farley, D., Ozair, S., Courville, A., and Bengio, Y. Generative adversarial nets. *NIPS'14*, 2014a.
- Goodfellow, I. J., Shlens, J., and Szegedy, C. Explaining and harnessing adversarial examples. *arXiv preprint arXiv:1412.6572*, 2014b.
- Haarnoja, T., Zhou, A., Abbeel, P., and Levine, S. Soft actor-critic: Off-policy maximum entropy deep reinforcement learning with a stochastic actor. In *ICML*, 2018.
- Hamidieh, K. A data-driven statistical model for predicting the critical temperature of a superconductor. *Computational Materials Science*, 154:346 – 354, 2018. ISSN 0927-0256. doi: <https://doi.org/10.1016/j.commatsci.2018.07.052>. URL <http://www.sciencedirect.com/science/article/pii/S0927025618304877>.
- Hansen, N. The CMA evolution strategy: A comparing review. In Lozano, J. A., Larrañaga, P., Inza, I., and Bengoetxea, E. (eds.), *Towards a New Evolutionary Computation - Advances in the Estimation of Distribution Algorithms*, volume 192 of *Studies in Fuzziness and Soft Computing*, pp. 75–102. Springer, 2006. doi: 10.1007/3-540-32494-1\_4. URL [https://doi.org/10.1007/3-540-32494-1\\_4](https://doi.org/10.1007/3-540-32494-1_4).
- Hill, A., Raffin, A., Ernestus, M., Gleave, A., Kanervisto, A., Traore, R., Dhariwal, P., Hesse, C., Klimov, O., Nichol, A., Plappert, M., Radford, A., Schulman, J., Sidor, S., and Wu, Y. Stable baselines. <https://github.com/hill-a/stable-baselines>, 2018.
- Hoburg, W. and Abbeel, P. Geometric programming for aircraft design optimization. volume 52, 04 2012. ISBN 978-1-60086-937-2. doi: 10.2514/6.2012-1680.
- Jacot, A., Gabriel, F., and Hongler, C. Neural tangent kernel: Convergence and generalization in neural networks. *arXiv preprint arXiv:1806.07572*, 2018.
- Kim, H., Mnih, A., Schwarz, J., Garnelo, M., Eslami, A., Rosenbaum, D., Vinyals, O., and Teh, Y. W. Attentive neural processes. In *International Conference on Learning Representations*, 2019. URL <https://openreview.net/forum?id=SkE6PjC9KX>.
- Kingma, D. P. and Ba, J. Adam: A method for stochastic optimization. In Bengio, Y. and LeCun, Y. (eds.), *3rd International Conference on Learning Representations, ICLR 2015, San Diego, CA, USA, May 7-9, 2015, Conference Track Proceedings*, 2015. URL <http://arxiv.org/abs/1412.6980>.
- Kingma, D. P. and Welling, M. Auto-encoding variational bayes, 2013. URL <http://arxiv.org/abs/1312.6114>. cite arxiv:1312.6114.
- Kumar, A. and Levine, S. Model inversion networks for model-based optimization. *arXiv preprint arXiv:1912.13464*, 2019.
- Kumar, A., Zhou, A., Tucker, G., and Levine, S. Conservative q-learning for offline reinforcement learning. *arXiv preprint arXiv:2006.04779*, 2020.
- Levine, S., Kumar, A., Tucker, G., and Fu, J. Offline reinforcement learning: Tutorial, review, and perspectives on open problems. *arXiv preprint arXiv:2005.01643*, 2020.
- Liao, T., Wang, G., Yang, B., Lee, R., Pister, K., Levine, S., and Calandra, R. Data-efficient learning of morphology and controller for a microrobot. In *2019 IEEE International Conference on Robotics and Automation*, 2019. URL <https://arxiv.org/abs/1905.01334>.
- Mirhoseini, A., Goldie, A., Yazgan, M., Jiang, J., Songhori, E., Wang, S., Lee, Y.-J., Johnson, E., Pathak, O., Bae, S., et al. Chip placement with deep reinforcement learning. *arXiv preprint arXiv:2004.10746*, 2020.
- Peters, J. and Schaal, S. Reinforcement learning by reward-weighted regression for operational space control. In *Proceedings of the 24th International Conference on Machine Learning, ICML '07*, 2007.
- Rubinstein, R. Y. Optimization of computer simulation models with rare events. *European Journal of Operations Research*, 99:89–112, 1996.
- Rubinstein, R. Y. and Kroese, D. P. *The Cross Entropy Method: A Unified Approach To Combinatorial Optimization, Monte-carlo Simulation (Information Science and Statistics)*. Springer-Verlag, Berlin, Heidelberg, 2004. ISBN 038721240X.
- Santurkar, S., Ilyas, A., Tsipras, D., Engstrom, L., Tran, B., and Madry, A. Image synthesis with a single (robust) classifier. In Wallach, H. M., Larochelle, H., Beygelzimer, A., d’Alché-Buc, F., Fox, E. B., and Garnett, R. (eds.), *Advances in Neural Information Processing Systems 32: Annual Conference on Neural Information Processing Systems 2019, NeurIPS 2019, 8-14 December 2019, Vancouver, BC, Canada*, pp. 1260–1271, 2019.
- Sarkisyan, K. S., Bolotin, D. A., Meer, M. V., Usmanova, D. R., Mishin, A. S., Sharonov, G. V., Ivankov, D. N., Bozhanova, N. G., Baranov, M. S., Soylemez, O., Bogatyreva, N. S., Vlasov, P. K., Egorov, E. S., Logacheva, M. D., Kondrashov, A. S., Chudakov, D. M., Putintseva, E. V., Mamedov, I. Z., Tawfik, D. S., Lukyanov, K. A., and Kondrashov, F. A. Local fitness landscape of the green fluorescent protein. *Nature*, 533 (7603):397–401, May 2016. ISSN 1476-4687. doi: 10.1038/nature17995. URL <https://doi.org/10.1038/nature17995>.

- Schulman, J., Wolski, F., Dhariwal, P., Radford, A., and Klimov, O. Proximal policy optimization algorithms. *CoRR*, abs/1707.06347, 2017. URL <http://arxiv.org/abs/1707.06347>.
- Shahriari, B., Swersky, K., Wang, Z., Adams, R. P., and de Freitas, N. Taking the human out of the loop: A review of bayesian optimization. *Proceedings of the IEEE*, 104: 148–175, 2016.
- Snoek, J., Larochelle, H., and Adams, R. P. Practical bayesian optimization of machine learning algorithms. In *Proceedings of the 25th International Conference on Neural Information Processing Systems - Volume 2*, NIPS’12, 2012. URL <http://dl.acm.org/citation.cfm?id=2999325.2999464>.
- Snoek, J., Rippel, O., Swersky, K., Kiros, R., Satish, N., Sundaram, N., Patwary, M., Prabhat, M., and Adams, R. Scalable bayesian optimization using deep neural networks. In *Proceedings of the 32nd International Conference on Machine Learning*. PMLR, 2015.
- Thomas, P., Theodorou, G., and Ghavamzadeh, M. High-confidence off-policy evaluation. In *Proceedings of the AAAI Conference on Artificial Intelligence*, volume 29, 2015.
- Trabucco, B., Geng, X., Kumar, A., and Levine, S. Design-bench: Benchmarks for data-driven offline model-based optimization, 2021. URL <https://github.com/brandontrabucco/design-bench>.
- Tramèr, F., Kurakin, A., Papernot, N., Goodfellow, I. J., Boneh, D., and McDaniel, P. D. Ensemble adversarial training: Attacks and defenses. In *6th International Conference on Learning Representations, ICLR 2018, Vancouver, BC, Canada, April 30 - May 3, 2018, Conference Track Proceedings*. OpenReview.net, 2018. URL <https://openreview.net/forum?id=rkZvSe-RZ>.
- Williams, R. J. Simple statistical gradient-following algorithms for connectionist reinforcement learning. *Mach. Learn.*, 8:229–256, 1992a. doi: 10.1007/BF00992696. URL <https://doi.org/10.1007/BF00992696>.
- Williams, R. J. Simple statistical gradient-following algorithms for connectionist reinforcement learning. *Machine Learning*, 8(3-4):229–256, May 1992b.
- Wilson, J. T., Moriconi, R., Hutter, F., and Deisenroth, M. P. The reparameterization trick for acquisition functions. *CoRR*, abs/1712.00424, 2017. URL <http://arxiv.org/abs/1712.00424>.
- Zoph, B. and Le, Q. V. Neural architecture search with reinforcement learning. 2017. URL <https://arxiv.org/abs/1611.01578>.

# Appendices

## A. Method Details

### A.1. Ablation of $\tau$

Equation 5 introduces a hyperparameter  $\tau$ , that controls how conservative the function  $\hat{f}_\theta(\mathbf{x})$  is during training. In this section, we provide an ablation study showing the sensitivity of COMs to this hyperparameter  $\tau$ . In this experiment, in order to demonstrate the relationship between the parameter  $\tau$ , and the stability of performance more clearly, we generate adversarial samples  $\mu(\mathbf{x})$  more aggressively by using 20 gradient ascent steps from each datapoint. This setting is a little different from our results in Table 1, where we find that generating adversarial samples  $\mu(\mathbf{x})$  by using a single gradient step from each datapoint suffices to obtain good performance while also being compute-wise less intensive. We set  $\beta = 0.0$  (Equation 4) in this experiment in order to test the affect of  $\tau$  in isolation of other confounding factors. As shown in Figure 6, we vary the parameter  $\tau$  from 0.5 to 0.001 and visualize the performance of solutions found by COMs as a function of the iteration of gradient ascent. Figure 6 demonstrates that increasing  $\tau$  can improve the stability of solutions found by COMs, but if  $\tau$  is large, solutions may converge too slowly. We empirically find an intermediate value of  $\tau = 0.05$  is appropriate universally, and effective on a wide range of offline MBO tasks, and we utilize this setting universally to obtain results in Table 1.

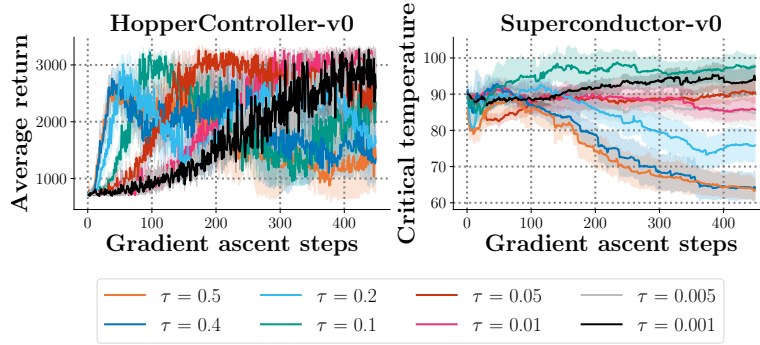


Figure 6. **Ablation of sensitivity and universality of  $\tau$ .** In each of the two plots, we instantiate COMs on the HopperController-v0 and Superconductor-v0 tasks, and vary  $\tau$  that controls the degree to which  $\hat{f}_\theta$  conservatively estimates the ground truth. The x-axis denotes the number of gradient ascent steps taken to update the design  $\mathbf{x}^*$  to maximize  $\hat{f}_\theta$ , and the y-axis indicates the resulting values of the ground truth function  $y$ , which remains unobserved by the COMs algorithm during training, and only serves as an ablative visualization. The results demonstrate that increasing  $\tau$  results in improved stability, at the expense of slower convergence. A value of  $\tau = 0.05$  is an appropriate *universal* choice of  $\tau$ .

### A.2. Optimization with Trust-Region Gradient Ascent

As per Equation 4, COMs updates performs gradient ascent on inputs  $\mathbf{x}$ , initialized from a particular  $\mathbf{x}_0 \in \mathcal{D}$ . This gradient ascent procedure utilizes a “trust-region” objective as restated below:

$$\begin{aligned} \forall t \in [T], \mathbf{x}_0 \in \mathcal{D}; \quad \mathbf{x}_{t+1} &= \mathbf{x}_t + \eta \nabla_{\mathbf{x}} \mathcal{L}_{\text{opt}}(\mathbf{x}) \big|_{\mathbf{x}=\mathbf{x}_t} \\ \text{where } \mathcal{L}_{\text{opt}}(\mathbf{x}) &:= \hat{f}_\theta^*(\mathbf{x}) - \beta \hat{f}_\theta^*(\mathbf{x} + \eta \nabla_{\mathbf{x}} \hat{f}_\theta^*(\mathbf{x})). \end{aligned} \quad (7)$$

The value of  $\beta$  here is technically a hyperparameter, and we find  $\beta = 0.9$  to be an appropriate choice *universally* across all the tasks. One practical consideration of this style of update is that the term  $\mathbf{x} + \eta \nabla_{\mathbf{x}} \hat{f}_\theta^*(\mathbf{x})$  depends on the current solution particles  $\mathbf{x}$ , and thus the gradient  $\nabla_{\mathbf{x}} \mathcal{L}_{\text{opt}}(\mathbf{x})$  contains a second-order term (i.e., Hessian of the function  $\hat{f}_\theta$  with respect to  $\mathbf{x}$ ). We empirically found that accounting for this second-order dependency is crucial and ignoring it leads to diminishing performance. Finally, a last consideration of this objective is how to tune the value of  $\beta$ . First note that in the formulation above,  $\beta$  always takes a value in a bounded interval  $[0, 1]$ :  $\beta \in [0, 1]$ . This is because any value of  $\beta$  outside this interval does not maximize the function  $\hat{f}_\theta(\mathbf{x})$  and instead attempts to reduce its value in an overall sense. In practice, a coarse search in intervals of 0.1 was enough in our experiments to identify a *universal* value of  $\beta$ .



Hyperparameter	Value
Number of epochs to train $\hat{f}_\theta$	500
$T$ (Number of gradient ascent steps using Equation 4)	450
$\alpha$ learning rate (used to optimize Equation 5 via dual gradient descent)	0.05
$\tau$ in Equation 5	0.05
$\beta$ in Equation 4	0.9
Number of steps used to generate adversarial samples $\mu(\mathbf{x})$ in Equation 5	1
$\eta$ in Equation 4	0.01

Table 2. **Hyperparameters for COMs.** All hyperparameters are kept constant across all tasks in COMs.

### A.3. Implementation details

In addition to various considerations from Sections 3.3 and 3.4, one important implementation detail of COMs is to normalize the inputs ( $\mathbf{x}$ ) and outputs ( $y$  values) for training the conservative model,  $\hat{f}_\theta(\mathbf{x})$ . Our motivation for using normalization was simple: Since the input and output ranges and modalities of various tasks we evaluated on in Table 1 is very different from each other, in order to be able to use a *uniform* set of hyperparameters for COMs, it is necessary to normalize both the inputs  $\mathbf{x}$  and outputs  $y$  to the same range. Following standard normalization practices, we normalized  $\mathbf{x}$  and  $y$  such that the resulting first and second moments match those of a unit Gaussian distribution. In practice, this means collecting all objective values from the training dataset into a vector  $Y \in \mathbb{R}^{N \times 1}$ , evaluating the sample mean  $\hat{\mu} = \text{mean}(Y)$  and sample standard deviation  $\hat{\sigma} = \text{std}(Y - \hat{\mu})$ . A similar procedure is used for calculating the sample mean and sample standard deviation of  $\mathbf{x}$ . The objective values and inputs are then normalized by subtracting their sample mean and dividing by their sample standard deviation  $y \leftarrow (y - \hat{\mu})/\hat{\sigma}$ . This normalization allows COMs to use the uniform set of hyperparameters, which we mention explicitly, in Table 2.

### A.4. Trust-Region Gradient Descent (Equation 4) and Equation 3

#### A.4.1. DOES EQUATION 4 OUTFRAN THE REGION DEFINED BY $\mu(\mathbf{x})$ , AS SHOWN IN TABLE 2?

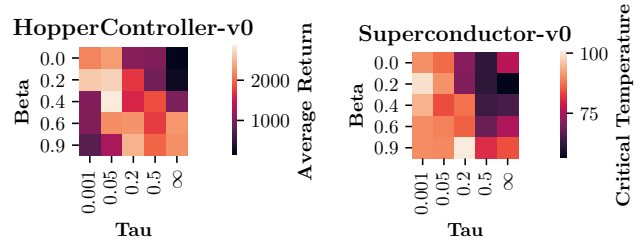
In this section, we present an empirical analysis that shows that even when 450 steps of Equation 4 are used, the learned conservative model,  $\hat{f}(\mathbf{x})$  satisfies the conservatism constraint satisfied by  $\mu(\mathbf{x})$  during training, i.e.,  $\hat{f}(\mathbf{x}^*) - f(\mathbf{x}_0) \leq \tau$ , where  $\mathbf{x}^*$  denotes the point found by the trust-region optimizer and  $\mathbf{x}_0$  is the initial point for Eqn. 4. For e.g., on HopperController, we find  $\hat{f}(\mathbf{x}^*) - f(\mathbf{x}_0) = 1.18$  while  $\tau = 2.0$  and on AntMorphology,  $\hat{f}(\mathbf{x}^*) - f(\mathbf{x}_0) = 0.39$  while  $\tau = 2.0$ . Thus the trust-region optimizer “**does not outrun**” the possible  $\mathbf{x}$  values for which the function  $\hat{f}(\mathbf{x})$  satisfies the conservatism constraint.

#### A.4.2. CAN COMS UTILIZE EQUATION 4 FOR COMPUTING $\mu(\mathbf{x})$ , THEREBY UNIFYING THE TWO PROCEDURES?

We now turn to answering the question if COMs can utilize Equation 4 used to compute  $\mathbf{x}^*$ , to also compute  $\mu(\mathbf{x})$ , thus unifying the two procedures. To empirically demonstrate that this is possible, we perform an experiment on two tasks and find that *COMs perform equally well* when the trust-region procedure in Equation 4 replaces  $\mu(\mathbf{x})$  in Equation 3 (while training  $\hat{f}^*$ ): HopperController:  $2801.4 \pm 282.0$  vs  $2864.5 \pm 535.0$  for base COMs; AntMorphology:  $443.1 \pm 8.9$  vs  $442.1 \pm 8.3$  for base COMs.

#### A.4.3. ABLATION STUDY OF $\tau$ (EQUATION 5) VS $\beta$ (EQUATION 4)

Finally, we present an ablation to understand the relative roles played by  $\beta$  and  $\tau$  in ensuring conservatism in COMs. While these hyperparameters are used in two different scenarios:  $\tau$  is used to train  $\hat{f}(\mathbf{x})$ ,  $\beta$  is used to find  $\mathbf{x}^*$ , we note that they might appear to serve a similar functionality of preventing the optimizer from finding out-of-distribution designs by controlling the learned model that is being optimized ( $\tau$ ) or by preventing the optimizer from going too far away from the training data ( $\beta$ , trust-region). To understand the relative impacts of  $\tau$  and  $\beta$ , we ran COMs with different values of  $\tau$  and  $\beta$  and plot the resulting performance



on a heatmap for two domains (left: HopperController (HC), right: Superconductor (SC)). We find that the contribution of  $\tau$  is crucial in COMs. For e.g., a specific value of  $\tau$  can generally attain reasonably good performance agnostic of  $\beta$  in both cases (HopperController: 0.05, SuperConductor: 0.001/0.05), whereas simply using Equation 4 with a standard objective model ( $\tau = \infty$ ) which is trained only with supervised regression and not conservatively, doesn't attain the best results across  $\beta$  values, indicating that  $\tau$  plays an important role in attaining good performance.

## B. Proof of Theorem 1

In this section, we provide a proof for Theorem 1 and show that the conservative training by performing gradient descent on  $\theta$  with respect to the objective in Equation 6 (restated below in a more convenient form as Equation 8) indeed obtains a conservative model of the actual objective function. Note that  $\bar{\mathcal{D}}(\mathbf{x}'|\mathbf{x})$  denotes a smoothed Dirac-delta distribution centered at  $\mathbf{x}$ , which can be obtained by adding random noise to a given  $\mathbf{x}$ .

$$\mathcal{L}(\theta; \mu, \bar{\mathcal{D}}) := \alpha \left( \mathbb{E}_{\mathbf{x}_0 \sim \bar{\mathcal{D}}, \mathbf{x}_T \sim \mu(\mathbf{x}_T|\mathbf{x}_0)} [\hat{f}_\theta(\mathbf{x}_T)] - \mathbb{E}_{\mathbf{x} \sim \bar{\mathcal{D}}, \mathbf{x}_T \sim \bar{\mathcal{D}}(\mathbf{x}_T|\mathbf{x}_0)} [\hat{f}_\theta(\mathbf{x}_T)] \right) + \underbrace{\frac{1}{2} \mathbb{E}_{\mathbf{x}_0 \sim \bar{\mathcal{D}}, (\mathbf{x}, y) \sim \bar{\mathcal{D}}(\mathbf{x}|\mathbf{x}_0)} \left[ \left( \hat{f}_\theta(\mathbf{x}) - y \right)^2 \right]}_{:= (\wedge)}. \quad (8)$$

We now restate a formal version of Theorem 1 (including correcting a typo from the informal version in the main paper, where the argument of the left hand side of the expression was denoted as  $\mathbf{x}'$  instead of  $\mathbf{x}''$ ), and then provide a proof. We make an additional assumption that the neural tangent kernel,  $\mathbf{G}_f^k(\mathbf{x}, \mathbf{x}')$ , is semi-positive definite.

**Theorem 2** (Formal version of Theorem 1). *Assume that  $\hat{f}_\theta(\mathbf{x})$  is trained by performing gradient descent on  $\theta$  with respect to the objective  $\mathcal{L}(\theta; \mu, \bar{\mathcal{D}})$  in Equation 8 with a learning rate  $\eta$ . The parameters in step  $k$  of gradient descent are denoted by  $\theta^k$ , and let the corresponding conservative model be denoted as  $\hat{f}_\theta^k$ . Let  $\mathbf{G}$ ,  $\mu$ ,  $\hat{L}$ ,  $L$ ,  $\bar{\mathcal{D}}$  be defined as discussed above. Then, under assumptions listed above,  $\forall \mathbf{x} \in \mathcal{D}, \mathbf{x}'' \in \mathcal{X}$ , the conservative model at iteration  $k+1$  of training satisfies:*

$$\hat{f}_\theta^{k+1}(\mathbf{x}'') := \max \left\{ \hat{f}_\theta^{k+1}(\mathbf{x}) - \hat{L} \|\mathbf{x}'' - \mathbf{x}\|_2, \tilde{f}_\theta^{k+1}(\mathbf{x}'') - \eta \alpha \mathbb{E}_{\mathbf{x} \sim \bar{\mathcal{D}}, \mathbf{x}' \sim \mu} [\mathbf{G}_f^k(\mathbf{x}'', \mathbf{x}')] + \eta \alpha \mathbb{E}_{\mathbf{x} \sim \bar{\mathcal{D}}, \mathbf{x}' \sim \bar{\mathcal{D}}} [\mathbf{G}_f^k(\mathbf{x}'', \mathbf{x}')] \right\},$$

where  $\tilde{f}_\theta^{k+1}(\mathbf{x}'')$  is the resulting  $(k+1)$ -th iterate of  $\hat{f}_\theta$  if conservative training were not used. Thus, if  $\alpha$  is sufficiently large, the expected value of the asymptotic function,  $\hat{f}_\theta := \lim_{k \rightarrow \infty} \hat{f}_\theta^k$ , on inputs  $\mathbf{x}_T$  found by the optimizer, lower-bounds the value of the true function  $f(\mathbf{x}_T)$ :

$$\mathbb{E}_{\mathbf{x}_0 \sim \mathcal{D}, \mathbf{x}_T \sim \mu(\mathbf{x}_T|\mathbf{x}_0)} [\hat{f}_\theta(\mathbf{x}_T)] \leq \mathbb{E}_{\mathbf{x}_0 \sim \mathcal{D}, \mathbf{x}_T \sim \mu(\mathbf{x}_T|\mathbf{x}_0)} [f(\mathbf{x})].$$

*Proof.* For proving the first part of the theorem, we first derive the expression for the gradient of  $\mathcal{L}(\theta; \mu, \bar{\mathcal{D}})$  with respect to  $\theta$ , and denote the  $y$ -value for a given  $\mathbf{x}$  as a deterministic function  $y(\mathbf{x})$ . Our proof can directly be extended to a non-deterministic  $y(\mathbf{x})$  with an additional integral over  $y$  values, but we stick to deterministic  $y(\mathbf{x})$  for simplicity.

$$\nabla_\theta \mathcal{L}(\theta; \mu, \bar{\mathcal{D}}) = \alpha \int (\bar{\mathcal{D}}(\mathbf{x}_0) \mu(\mathbf{x}|\mathbf{x}_0) - \bar{\mathcal{D}}(\mathbf{x}_0) \bar{\mathcal{D}}(\mathbf{x}|\mathbf{x}_0)) \nabla_\theta \hat{f}_\theta(\mathbf{x}) d\mathbf{x}_0 d\mathbf{x} + \int \bar{\mathcal{D}}(\mathbf{x}_0) \bar{\mathcal{D}}(\mathbf{x}|\mathbf{x}_0) (f_\theta(\mathbf{x}) - y(\mathbf{x})) \nabla_\theta \hat{f}_\theta(\mathbf{x}) d\mathbf{x} d\mathbf{x}_0.$$

At any iteration  $k$  of gradient descent, the next parameter iterate  $\theta^{k+1}$  are obtained via,  $\theta^{k+1} = \theta^k - \eta \nabla_\theta \mathcal{L}(\theta; \mu, \bar{\mathcal{D}})$ . Using this relation, and making an approximate linearization assumption on the non-linear function  $\hat{f}_\theta^k$  for a small learning rate  $\eta \ll 1$  under the assumption of the neural tangent kernel (NTK) (Jacot et al., 2018) regime, which models the behavior of deep neural networks in the infinite-width limit, we obtain the expression for the next function value:  $\hat{f}_\theta^{k+1}(\mathbf{x}'')$ :

$$\begin{aligned} \hat{f}_\theta^{k+1}(\mathbf{x}'') &\approx \hat{f}_\theta^k(\mathbf{x}'') + (\theta^{k+1} - \theta^k)^T \nabla_\theta \hat{f}_\theta^k(\mathbf{x}'') \\ &= \underbrace{\hat{f}_\theta^k(\mathbf{x}'') + \eta \mathbb{E}_{\mathbf{x} \sim \bar{\mathcal{D}}, \mathbf{x}' \sim \bar{\mathcal{D}}} \left[ \left( y(\mathbf{x}') - \hat{f}_\theta^k(\mathbf{x}') \right) \mathbf{G}_f^k(\mathbf{x}'', \mathbf{x}') \right]}_{:= (*)} - \underbrace{\left( \eta \alpha \mathbb{E}_{\mathbf{x} \sim \bar{\mathcal{D}}, \mathbf{x}' \sim \mu} [\mathbf{G}_f^k(\mathbf{x}'', \mathbf{x}')] - \eta \alpha \mathbb{E}_{\mathbf{x} \sim \bar{\mathcal{D}}, \mathbf{x}' \sim \bar{\mathcal{D}}} [\mathbf{G}_f^k(\mathbf{x}'', \mathbf{x}')] \right)}_{:= \Delta(\mathbf{x}'')}, \end{aligned}$$

where the expression marked as  $(*)$  denotes the  $(k+1)$ -th iterate of the function, under gradient descent on just the mean-squared error  $(f(\mathbf{x}) - y)^2$  term, marked as  $(\wedge)$  in Equation 8. Noting that the theorem statement denotes the term  $(*)$  as  $\tilde{f}_\theta^{k+1}(\mathbf{x}'')$ , we obtain our first desired result. To obtain the first argument of the max in the theorem statement, note that if

the function  $\hat{f}_\theta^{k+1}$  is  $\hat{L}$ -Lipschitz, the value at  $\mathbf{x}''$  cannot be smaller than  $\hat{f}_\theta^{k+1}(\mathbf{x}) - \hat{L}\|\mathbf{x} - \mathbf{x}''\|_2$ , and hence the maximum over the two terms.

For proving the second part of the theorem statement, observe that if we can show that in expectation over  $\mathbf{x}'' \sim \mu(\mathbf{x}_T); \mu(\mathbf{x}_T) := \int_{\mathbf{x}_0} \bar{\mathcal{D}}(\mathbf{x}_0) \mu(\mathbf{x}_T | \mathbf{x}_0) d\mathbf{x}_0$ , the quantity  $\Delta(\mathbf{x}'')$  is positive, then our argument is complete since we have shown that each step of gradient descent on  $\theta$  reduces the value of  $\mathbb{E}_{\mathbf{x}_0 \sim \bar{\mathcal{D}}, \mathbf{x}_T \sim \mu(\mathbf{x}_T | \mathbf{x}_0)}[\hat{f}_\theta^k(\mathbf{x}_T)]$  by a positive quantity by virtue of training with Equation 8 as compared to only training  $\theta$  with standard squared error ( $\wedge$ ). Thus, if  $\mathbb{E}_{\mathbf{x}_0 \sim \bar{\mathcal{D}}, \mathbf{x}_T \sim \mu(\mathbf{x}_T | \mathbf{x}_0)}[\Delta^k(\mathbf{x}_T)]$  is positive for all gradient descent steps  $k$ , we obtain the desired lower-bound condition as  $k \rightarrow \infty$ . As an additional detail, note that we assumed  $\hat{L} \gg L$  (i.e. the Lipschitz constant of  $\hat{f}_\theta(\mathbf{x})$  is sufficiently larger than that of  $f(\mathbf{x})$ ). This condition handles the boundary case when the predictions  $\hat{f}_\theta^{k+1}(\mathbf{x}')$  get lower-bounded under the first argument of max in the first part of Theorem 2 due to the Lipschitz condition:  $\hat{f}_\theta^{k+1}(\mathbf{x}) - \hat{L}\|\mathbf{x}' - \mathbf{x}\|_2$ .

Finally, we fill in the missing piece that show  $\mathbb{E}_{\mathbf{x}_0 \sim \bar{\mathcal{D}}, \mathbf{x}_T \sim \mu(\mathbf{x}_T | \mathbf{x}_0)}[\Delta^k(\mathbf{x}_T)]$  is positive for each  $k$ . Under the assumption that the neural tangent kernel  $\mathbf{G}^k(\mathbf{x}, \mathbf{x}')$  is semi-positive definite for all  $k$ , we can express:

$$\begin{aligned} \mathbb{E}_{\mathbf{x}_0 \sim \bar{\mathcal{D}}, \mathbf{x}_T \sim \mu(\mathbf{x}_T | \mathbf{x}_0)}[\Delta^k(\mathbf{x}_T)] &:= \eta\alpha \int_{\mathbf{x}, \mathbf{x}_0, \mathbf{x}', \mathbf{x}_T} [\bar{\mathcal{D}}(\mathbf{x})\mu(\mathbf{x}' | \mathbf{x}) - \bar{\mathcal{D}}(\mathbf{x})\bar{\mathcal{D}}(\mathbf{x}' | \mathbf{x})] \bar{\mathcal{D}}(\mathbf{x}_0)\mu(\mathbf{x}_T | \mathbf{x}_0) \mathbf{G}_f^k(\mathbf{x}', \mathbf{x}_T) \\ &= \eta\alpha \int_{\mathbf{x}_0} \bar{\mathcal{D}}(\mathbf{x}_0) \int_{\mathbf{x}} \bar{\mathcal{D}}(\mathbf{x}) \int_{\mathbf{x}', \mathbf{x}_T} [\mu(\mathbf{x}' | \mathbf{x}) - \bar{\mathcal{D}}(\mathbf{x}' | \mathbf{x})] \mu(\mathbf{x}_T | \mathbf{x}_0) \mathbf{G}_f^k(\mathbf{x}', \mathbf{x}_T) \end{aligned}$$

By now writing the above in matrix form, we note that the RHS of the above equation has the same structure as the second term in the RHS of Equation 14 in Kumar et al. (2020), and furthermore since  $\mathbf{G}_f^k$  is positive semi-definite, it satisfies the required conditions for Equation 14 and Theorem D.1 from Kumar et al. (2020) to be applicable. Thus, exactly following the proof of Theorem D.1 in Kumar et al. (2020) for the linear function approximation case in reinforcement learning, with the following substitutions:  $P_F := \mathbf{G}_f^k(\cdot, \mathbf{x}_T)$  (i.e., a column of the kernel Gram-matrix for a fixed value of the second argument) and  $a = \mathbf{x}_T, s = \mathbf{x}_0$ , we can show that  $\mathbb{E}_{\mathbf{x}_0 \sim \bar{\mathcal{D}}, \mathbf{x}_T \sim \mu(\mathbf{x}_T | \mathbf{x}_0)}[\Delta^k(\mathbf{x}_T)] \geq 0$ , thus finishing our argument.  $\square$

## C. Network Details

In each of our experiments, we train a neural network  $\hat{f}_\theta$  to approximate the ground truth score function of an offline MBO task, where  $\theta$  represents the weights of the model. Distinct from prior methods based on generative models (Kumar & Levine, 2019; Brookes et al., 2019) we are able to utilize the same neural network architecture for representing the learned model,  $\hat{f}_\theta(\mathbf{x})$  across all MBO tasks. This architecture is a three-layer neural network with two hidden layers of size 2048, followed by Leaky ReLU activation functions with a leak of 0.3. Each neural network  $\hat{f}_\theta$  has an output layer that predicts a Gaussian distribution over potential objective values  $y$  by predicting both the mean  $\mu_\theta(\mathbf{x})$  and log standard deviation  $\log \sigma_\theta(\mathbf{x})$  of that distribution. For numerical stability, the log standard deviation is passed through a softplus function (rather than an exponential) to obtain standard deviation. The neural network  $\hat{f}_\theta$  is trained to minimize negative log likelihood of observed data, using the default parameters of the Adam optimizer as discussed in Section 3.4.

## D. Tasks and Data Collection

The tasks from this paper are taken from Design-Bench (Trabucco et al., 2021), a work-in-progress benchmark for evaluating offline model based optimization methods. We provide a copy of the paper in the supplementary material. We detail the data collection steps used for creating each of the tasks in design-bench. We answer (1) where is the data from, and (2) what pre-processing steps are used?

### D.1. Superconductor-v0

Superconductor-v0 is inspired by recent work (Fannjiang & Listgarten, 2020) that applies offline MBO to optimize the properties of superconducting materials for high critical temperature. The data we provide in our benchmark is real-world superconductivity data originally collected by (Hamidieh, 2018), and subsequently made available to the public at the url <https://archive.ics.uci.edu/ml/datasets/Superconductivity+Data#>. The original dataset consists of superconductors featurized into vectors  $x_{\text{Superconductor}} \in \mathcal{R}^{81}$ . One issue with the original dataset is that the largest value of a single dimension in the dataset is 22590.0, which appears to cause learning instability. We follow (Fannjiang & Listgarten, 2020) and normalize each dimension of the design-space to have zero mean and unit variance. However, we deviate from

the remaining pre-processing steps in (Fannjiang & Listgarten, 2020). In order to promote task realism, we directly use the superconductivity data, whereas (Fannjiang & Listgarten, 2020) re-samples by collecting iid unit gaussian samples and labelling them with the task oracle function. This causes the scores in the dataset to correspond exactly to the scores provided by the oracle. No other domain in design-bench re-samples nor re-labels static data, so we omit it here for consistency.

## D.2. HopperController-v0

The HopperController task is one that we provide ourselves. The goal of this task is to design a set of weights for a neural network policy, in order to achieve high expected return when evaluating that policy. The data collected for HopperController was taken by training a three layer neural network policy with 64 hidden units and 5126 total weights on the Hopper-v2 MuJoCo task using Proximal Policy Optimization (Schulman et al., 2017). Specifically, we use the default parameters for PPO provided in stable baselines (Hill et al., 2018). The dataset we provide with this benchmark has 3200 unique weights. In order to collect this many, we run 32 experimental trials of PPO, where we train for one million steps, and save the weights of the policy every 10,000 environment steps. The policy weights are represented originally as a list of tensors. We first traverse this list and flatten each of the tensors, and we then concatenate each of these flattened tensors into a single training example  $x_{\text{Hopper}} \in \mathcal{R}^{5126}$ . The result is an optimization problem over neural network weights. After collecting these weights, we perform no additional pre-processing steps. In order to collect scores we perform a single rollout for each  $x$  using the Hopper-v2 MuJoCo environment. The horizon length for training and evaluation is limited to 1000 simulation time steps.

## D.3. AntMorphology-v0 & DKittyMorphology-v0

Both morphology tasks are collected by us with the same methodology. The goal of these tasks is to design the morphology of a quadrupedal robot—an ant or a D’Kitty—such that the agent is able to crawl quickly in a particular direction. In order to collect data for this environment, we create variants of the MuJoCo Ant and the ROBEL D’Kitty agents that have parametric morphologies. The goal is to determine a mapping from the morphology of the agent to the average return that an agent trained for a particular intended morphology achieves. We implement this by pre-training a neural network policy using SAC (Haarnoja et al., 2018). For both the Ant and the D’Kitty, we train agents for up to three million environments steps, and a maximum episode length of 1000, with all other settings as default. These agents are pre-trained for a fixed gold-standard morphology—the default morphology of the Ant and D’Kitty respectively. Each morphology task consists of samples obtained by adding Gaussian noise with standard deviation 0.02 for Ant and 0.01 for DKitty times the design-space range to the gold-standard morphology. We label each sampled morphology by averaging the return of 16 rollouts of length 100 of an agent with that morphology.

## E. Oracle Functions

We detail oracle functions for evaluating ground truth objective values for each of the tasks in Table 1.

### E.1. Superconductor-v0

The Superconductor-v0 oracle function is also a random forest regression model. The model we use is the model described by (Hamidieh, 2018). We borrow the hyperparameters described by them, and we use the Random Forest Regressor provided in scikit-learn. Similar to the setup for the previous two tasks, this oracle is trained on the entire static dataset, and the task is instantiated with a split percentile. Samples scoring at most in the 80th percentile are observed by an MBO algorithm, which allows for sampling *unobserved* points that score in the unobserved top 20 percent.

### E.2. HopperController-v0

Unlike the previously described tasks, HopperController-v0 and the remaining tasks implement an exact oracle function. For HopperController-v0 the oracle takes the form of a single rollout using the Hopper-v2 MuJoCo environment. The designs for HopperController-v0 are neural network weights, and during evaluation, a policy with those weights is instantiated—in this case that policy is a three layer neural network with 11 input units, two layers with 64 hidden units, and a final layer with 3 output units. The intermediate activations between layers are hyperbolic tangents. After building a policy, the Hopper-v2 environment is reset and the reward for 1000 time-steps is summed. That summed reward constitutes the score returned by the HopperController-v0 oracle. The limit of performance is the maximum return that an agent can achieve in Hopper-v2



over 1000 steps.

### **E.3. AntMorphology-v0 & DKittyMorphology-v0**

The final two tasks in design-bench use an exact oracle function, using the MuJoCo simulator. For both morphology tasks, the simulator performs 16 rollouts and averages the sum of rewards attained over them. Each task is accompanied by a pre-trained neural network policy. To perform evaluation, a morphology is passed to the Ant or D’Kitty MuJoCo environments respectively, and a dynamic-morphology agent is initialized inside these environments. These environments are very sensitive to small morphological changes, and exhibit a high degree of stochasticity as a result. To compensate for the increased stochasticity, we average returns over 16 rollouts.